

***K*-shell photoabsorption edge of a dense aluminum plasma**

B. K. Godwal,* A. Ng, and L. Da Silva

Department of Physics, University of British Columbia, Vancouver, British Columbia, Canada V6T 2A6

Y. T. Lee and D. A. Liberman

Department of Physics, Lawrence Livermore National Laboratory, Livermore, California 94550

(Received 2 May 1989)

A theoretical model for the calculation of the *K*-shell photoabsorption edge in a dense plasma is described. In the model, degeneracy and continuum lowering contributions due to free electrons and neighboring ions were treated as perturbations on the continuum and the bound state. These contributions were evaluated using first-principles solid-state methods. The model was used to interpret recently observed shifts in the *K*-shell photoabsorption-edge energy in shock-compressed aluminum. The validity of the model was further examined through comparisons with two average-atom, self-consistent-field calculations and an augmented-plane-wave calculation.

I. INTRODUCTION

Understanding the properties of matter at extreme conditions of pressure and temperature is not only of fundamental importance in the studies of plasmas, condensed matter, geophysics, and astrophysics but also of practical interest in inertial confinement fusion applications. Such states can be readily attained in shock compression of solids via hypervelocity impact,¹ nuclear explosion,¹ or laser-driven ablation.² This has led to extensive studies on the thermodynamic properties of high-density matter along the shock Hugoniot.¹ On the other hand, there exist few studies on the atomic properties such as electronic structure, ionization state, ionization potential, and ion correlation. Such properties are not mutually independent, and they are important for the computation of opacity and the generation of accurate equation of state data.

The first experiment to probe the atomic properties of a dense plasma was reported by Bradley *et al.*,³ in which the structure and position of the *K*-shell photoabsorption edge of chlorine was observed when a layer of KCl was radiatively preheated to a temperature of several electron volts and then compressed by a strong shock to several times solid density. The observed red shift in the chlorine *K* edge during the compression phase suggested pressure ionization of the $3p$ level. Experimental observations of ion-correlation effects in a dense plasma were later obtained by Hall *et al.*⁴ The plasma, produced in aluminum by colliding shocks driven by laser beams, reached a peak temperature of over 1 eV and densities of several times that of a solid. The short-range order within the plasma was determined from extended x-ray-absorption fine-structure (EXAFS) spectrum of the aluminum *K* absorption edge.

Recently, we reported on the observation of changes in the *K*-shell photoabsorption edge of aluminum as it was compressed by a laser-driven shock wave.⁵ During the rise in shock pressure, the aluminum *K* edge continued to shift to the red. Then, after the shock emerged at the free

surface of the target which began to decompress, the *K* edge was found to shift back towards its normal position. In an attempt to understand the observed effect of shock compression on the *K*-shell photoabsorption edge, a theoretical model was developed. The aim of this paper is to present a detailed description of the model and its application to dense aluminum plasmas, and to explore the effectiveness of the model compared with that of the relativistic average-atom models, HOPE⁶ and INFERNO,^{7,8} and the augmented-plane-wave (APW) calculation.⁹

Our starting point is the assumption that when an ion is placed in a dense plasma, its bound and continuum levels will be altered due to interactions with the surrounding free electrons and ions, and these changes are given by the degeneracy and continuum-lowering contributions.¹⁰ The model lacks self-consistency and ignores relaxation effects. However, such a phenomenological prescription allows us to calculate explicitly the dense-plasma effects at finite temperatures using solid-state methods. Specifically, the degeneracy contribution includes the chemical potential and the first- and second-order band-structure corrections to the energy of the free electron.¹¹ The continuum lowering contribution is computed from the linearized muffin-tin-orbital (LMTO) method of Skriver.¹² It should be noted that a simpler phenomenological approach to describe energy levels of an ion in a dense plasma was employed by Bradley *et al.*,¹³ who evaluated the dense-plasma effects using an ion-sphere model.

II. THEORETICAL FORMULATION

For a plasma with density ρ , temperature T , and average ionization state Z^* , the *K*-shell photoabsorption-edge energy is defined phenomenologically as

$$E_K(\rho, T) = E_{IK}(Z^*) + \Delta E_{\text{deg}}(\rho, T) + \Delta E_{\text{CL}}(\rho, T). \quad (1)$$

The first term E_{IK} is the average *K*-shell ionization energy of an isolated ion with charge Z^* . The degeneracy term ΔE_{deg} represents the energy of a free electron due to

partial degeneracy and interactions with other electrons and ions. Finally, the continuum-lowering contribution ΔE_{CL} represents the change in the energy of the bound-electron state due to screening of the ion core by neighboring free electrons and ions.

Accordingly, the first step towards calculating the K -edge energy requires the determination of the average ionization state Z^* of the plasma at a given density and temperature. In the literature, various prescriptions such as temperature-dependent Thomas-Fermi model,¹⁴ augmented-plane-wave (APW) methods,⁹ and complete screened Coulomb potential ionization equilibrium equation of state (CSCP-IEEOS) form of the modified Saha ionization theory^{15,16} have been used for the calculation of average ionization states. In the present work we employed the CSCP-IEEOS method as it includes high density effects such as lowering of ionization potentials, partition function cutoff, and pressure ionization. This method has also been used successfully to predict the normal valencies for different elements and to simulate qualitatively the valence transitions under pressure in yttrium and ytterbium. The average K -shell ionization energy for the dominant ions $E_{IK}(Z^*)$ is then obtained from detailed Hartree-Slater calculations¹⁷ (or Dirac Hartree-Slater theory for high- Z elements¹⁸).

The degeneracy term is computed from

$$\Delta E_{\text{deg}} = \mu - U_1 - U_2, \quad (2)$$

where μ is the chemical potential and is due to the fact that in order to add any new electron to the already occupied continuum fermion states, energy at least as high as that of the lowest unoccupied state is required. The use of μ ignores details of the distribution of the occupied states at finite temperature. This approximation is reasonable for temperature much less than the Fermi temperature. U_1 and U_2 are, respectively, the first- and second-order corrections to the energy of an electron in the continuum due to interactions with neighboring ions and free electrons. These different contributions to ΔE_{deg} are evaluated in the framework of the nearly-free-electron theory of Heine and Weaire,¹¹ with U_1 determined by zero-pressure condition and U_2 calculated using Ashcroft's empty-core pseudopotential¹⁹ and using the standard prescription of second-order perturbation theory. For aluminum at twofold compression, $\mu = 18.4$ eV, $U_1 = 30.71$ eV and $U_2 = 0.01$ eV.

The change in the binding energy due to continuum lowering ΔE_{CL} is approximated by the change in the energy of a valence atomic level when it becomes a band state. That is,

$$\Delta E_{CL} = E_B - E_A, \quad (3)$$

where E_B is the energy of the conduction-band electron in the solid lattice and E_A is the binding energy of the same electron in the isolated atom. E_A is obtained from Hartree-Slater calculations¹⁷ and E_B is computed with the LMTO package of Skriver.¹² The LMTO method evaluates the one-electron eigenvalues of an ordered solid within the local-density formulation of Kohn-Sham,²⁰ using Barth-Heidin exchange and correlation potentials.²¹

For aluminum, the calculations are carried out for the $3s^23p^1$ electronic configuration in the face-centered-cubic structure by including angular momentum states up to $l=3$. At a twofold compression, $E_B = -24.6$ eV and $E_A = -4.9$ eV.

III. APPLICATION TO ALUMINUM

Figure 1 shows the average ionization state Z^* of aluminum at normal density (2.7 g/cm^3) as a function of temperature, obtained from CSCP-IEEOS calculations.^{15,16} Thermal ionization begins to take effect at ~ 7.7 eV. At higher temperatures, Z^* increases rapidly. Below the temperature where thermal ionization occurs, the ionization state $Z^* = 3$ presented in Fig. 1 should be interpreted as the number of electrons outside of the core of an aluminum ion. At normal density, the wave functions of these electrons are not localized around a single ion, but are spread over many neighboring ions. The energy levels of these electrons also merge to form quasienergy bands. The K -shell ionization energy is then given as the energy needed to excite a K -shell electron to an unoccupied state in the energy bands. On the other hand, pressure ionization becomes important only at densities above four times solid density. In the range of temperature presented in Fig. 1, pressure ionization will cause Z^* to increase by 1 at a compression of $V/V_0 \approx 0.25$, where V and V_0 are the specific volumes under pressure and normal conditions.

Results of the Hartree-Slater calculations¹⁷ on the K -shell ionization energies of isolated ions of aluminum are given in Table I. The strong dependence of the K -shell ionization energy on the ion-charge state suggests that the accuracy of any model in calculating the K -shell photoabsorption edge energy in a dense plasma will be influenced by the accuracy of the ionization state calculations.

For the evaluation of the dense-plasma effects on the aluminum K -shell photoabsorption edge energy, the present model is applicable for shock compression up to

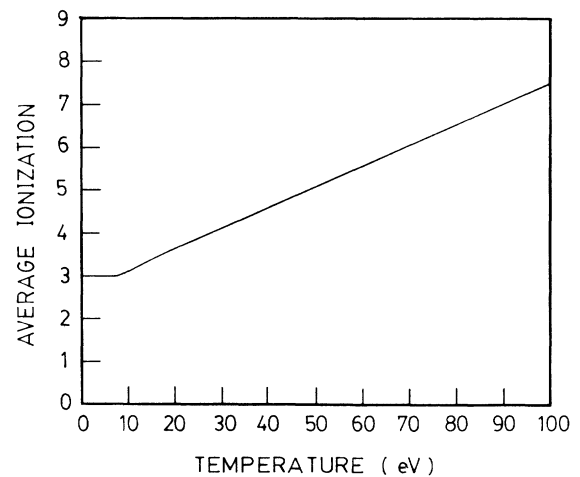


FIG. 1. Average ionization as a function of temperature at normal density.

TABLE I. K -shell ionization energies (in units of eV) of isolated aluminum ions.

Ions	E_{IK} (eV)
Al ¹⁺	1555.0
Al ²⁺	1568.6
Al ³⁺	1584.0
Al ⁴⁺	1629.8
Al ⁵⁺	1679.7
Al ⁶⁺	1733.4
Al ⁷⁺	1784.6
Al ⁸⁺	1854.6
Al ⁹⁺	1915.5
Al ¹⁰⁺	1980.9
Al ¹¹⁺	2063.1
Al ¹²⁺	2283.2

$V/V_0 \sim 0.35$. Beyond that the model becomes less accurate because of the lack of treatment of liquid disorder and the inability of the model to deal with the coupling of the core and conduction electrons. Results of our calculations of the degeneracy term (ΔE_{deg}), the continuum-lowering term (ΔE_{CL}) and the K -shell photoabsorption edge energy (E_K) are presented in Figs. 2, 3, and 4, respectively. For the range of temperature and density considered, the degeneracy contribution increases slowly with density but shows a much weaker dependence on temperature, whereas the continuum-lowering contribution varies only slightly with temperature or density. The increase in both ΔE_{deg} and ΔE_{CL} with temperature can be attributed to the increase in the average ionization state of aluminum above 8 eV (Fig. 1). Since pressure ionization remains ineffective within the range of compression of interest, the K -shell ionization energy of

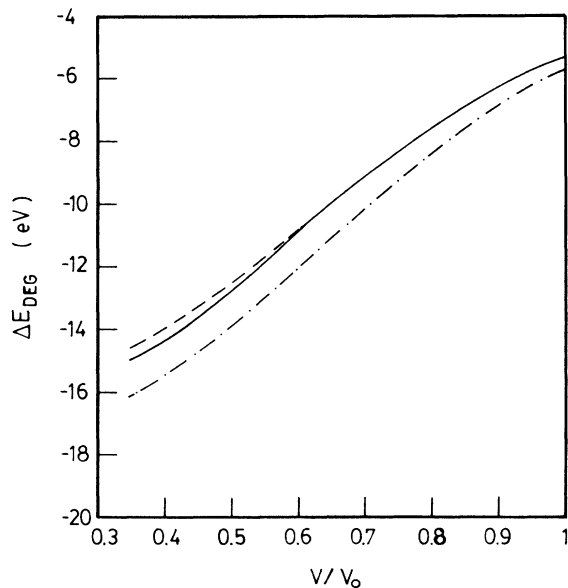


FIG. 2. ΔE_{deg} as a function of compression along the 0.1-eV curve (dashed line), 15-eV curve (dot-dashed line), and Hugoniot (solid line).

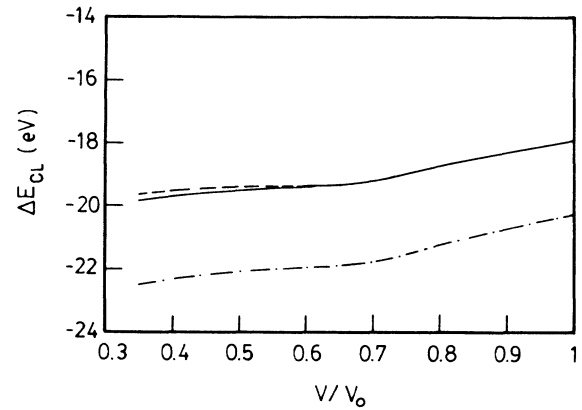


FIG. 3. ΔE_{CL} as a function of compression along the 0.1-eV curve (dashed line), 15-eV curve (dot-dashed line), and Hugoniot (solid line).

an isolated aluminum ion E_{IK} is independent of average density. For temperatures greater than 8 eV, thermal ionization raises the average ionization state above 3. At 15 eV, the average ionization state is 3.4 (Fig. 1) and the plasma will be dominated by Al³⁺ and Al⁴⁺ ions, with each of these species giving rise to its own K edge. For comparison purposes, all curves presented in Figs. 2 to 4 correspond to that for the Al³⁺ ions. The temperature and density dependences of the K -edge energy E_K reflect that of the component terms defined in Eq. (1). It should be noted that calculations have been made at 15 eV only

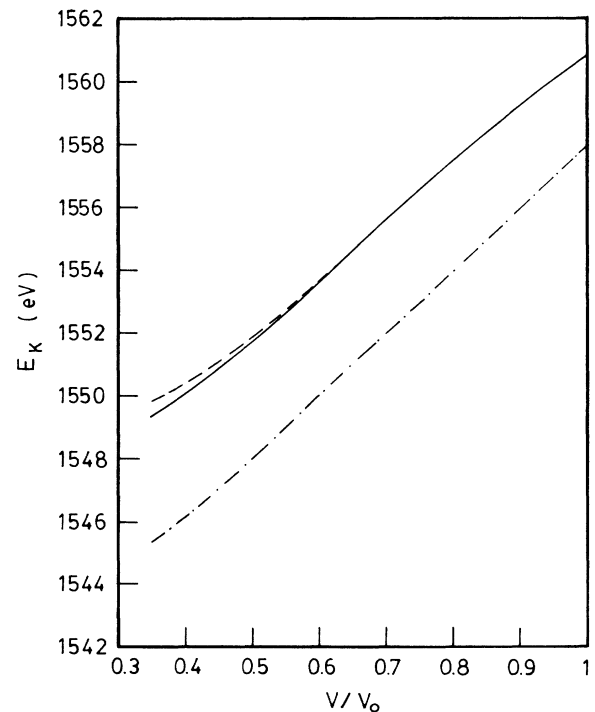


FIG. 4. E_K as a function of compression along the 0.1-eV curve (dashed line), 15-eV curve (dot-dashed line), and Hugoniot (solid line).

to assess approximately the temperature effect. The use of chemical potential in Eq. (2) at such a high temperature may become a poor estimate.

Figure 5 shows the calculated shift in the aluminum K edge (relative to its value at normal conditions) along the principal Hugoniot, compared with results of other theoretical models as well as recent experimental data. Details of the INFERNO, HOPE, and APW models have been described by Liberman,^{7,8} Rozsnyai,⁶ and McMahan and Ross,⁹ respectively. Both INFERNO and HOPE calculate the K -edge energy along the Hugoniot. The APW calculations have been carried out along the zero degree isotherm only. At twofold shock compression, the temperature will be about 1.2 eV. The finite temperature correction to the APW result is not known presently. Being a self-consistent solid-state model, the APW calculation yields the correct aluminum K -edge energy of 1560 eV at normal condition.²² On the other hand, the present model, INFERNO, and HOPE all predicted a different normal K -edge energy of 1560.8 eV, 1562.78 eV, and 1545.2 eV, respectively. Thus, we have considered only the change in the K -edge energy due to compression instead of its absolute value. The K -edge energy 1562.78 eV given by INFERNO is for the density of 3.40 g/cm^3 . However, we expect that the K -edge energy at normal condition would also have this value because INFERNO calculates a very small shift in K -edge energy at the compression up to $V/V_0=0.6$. We would also like to point out that the INFERNO calculation uses the transition state,²³ a state in which the occupation number of the K shell is 1.5 which is a halfway between the initial and final states of a photoionization transition. For the range of shock pressure considered, all models suggest a red-shift of the K edge under compression. However, the

dense plasma effects attributed by the various models differ substantially.

Measurements of the aluminum K -edge energy under shock compression were made using time-resolved, x-ray-absorption spectroscopy. In the experiment, aluminum foils of thicknesses 6, 9, and $25 \mu\text{m}$ were irradiated with a $0.53 \mu\text{m}$, 2.3 ns full width at half maximum (FWHM) laser pulse at an absorbed irradiance of $2.3 \times 10^{13} \text{ W/cm}^2$. The resulting laser ablation drove an intense shock wave into the target. The shock pressure was determined from shock transit time measurements by observing the onset of luminous emission from the free surface (back surface) of the target. The results showed good agreement with one-dimensional hydrodynamic simulations²⁴ which included multigroup radiation transport.²⁴ This yielded a good estimate of the density and temperature conditions in the target. To determine the K edge in the shocked material, x-ray emission from the aluminum plasma on target front side was used to backlight the target. This provided a continuum source in the spectral region (1545–1570 eV) around the aluminum K edge.²⁵ The transmitted x-ray spectrum was measured using a crystal spectrometer and x-ray streak camera system. Details of the experiment as well as the analysis of the change in the aluminum K edge during compression and decompression of the target have been described elsewhere.⁵ The data described in Fig. 5 represent the observed K edge at the time the laser-driven shock wave reached the free surface of the target. For the 9-, 16-, and $25\text{-}\mu\text{m}$ foils, the corresponding compressions are 0.82, 0.66, and 0.45, respectively. The uncertainty in the density is due to the finite accuracy of the shock speed measurement. The extent of the K edge shown represents the observed width of the edge. Two-dimensional hydrodynamic simulations⁵ have suggested that the observed width of the K edge could be attributed to the two-dimensional nature of the shock wave in the target and the K edge was given by the maximum red-shifted position. However, without a clear understanding of edge-broadening mechanisms, it remains difficult to identify definitively the exact location of the K edge within its observed width. The experimental data, lying within the region bounded by predictions from the various models, would suggest inadequacies in all models.

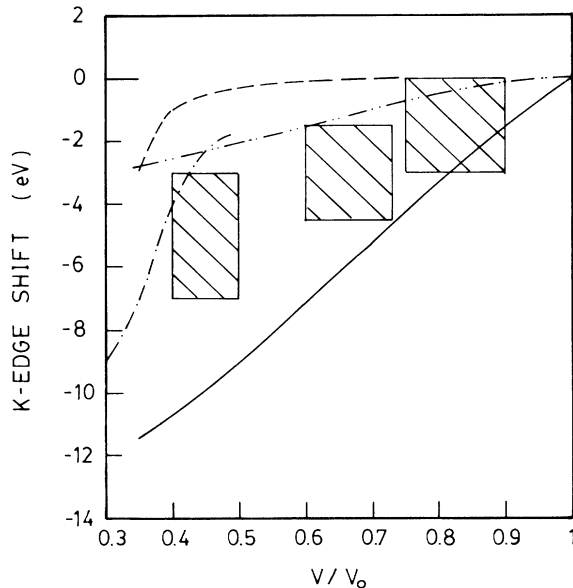


FIG. 5. Shift in the K -edge energy as a function of shock compression: present model (solid line), INFERNO (dashed line), HOPE (dot-dashed line), APW (dot-dot-dashed line), and experimental data (hatched area).

IV. DISCUSSIONS AND CONCLUSIONS

The model presented here attempts to treat dense-plasma effects using solid-state methods. The phenomenology used undoubtedly lacks self-consistence. The model considers only the ionization energy of a K -shell electron in an aluminum ion in the initial state and thus ignores effects of relaxation towards the final state in which the K -shell electron has been freed. It is also open to criticism that continuum lowering due to the screening of the ion core by neighboring ions and free electrons may only be effective for the loosely bound outer states but not for the tightly bound inner-shell levels. At present, it appears that the model gives an upper bound on the red-shift of the K -shell photoabsorption edge under compression.

On the other hand, calculations using the INFERNO, HOPE, or APW models seem to have underestimated the shift in the aluminum K edge. The HOPE code is based on an average-atom model which calculates single-particle energy levels and wave functions in a fully self-consistent manner using a Hartree-Slater potential. The electrons of the atom are confined inside a sphere with the radius determined by the matter density of a plasma. The wave functions of these electrons are calculated with the boundary condition which can broaden the excited levels into energy bands. The code computes a noninteger occupational number of the levels according to Fermi-Dirac statistics. Therefore, the K -edge energy obtained from HOPE represents the average K edge for all possible charge states in a plasma. However, for aluminum under shock compression, the electron temperatures are less than 7.0 eV at the compression discussed in Fig. 5. At these temperatures, both the HOPE code and the results in Fig. 1 clearly show that Al^{3+} is the only charge state with appreciable population in a plasma. Therefore, the K -edge energies calculated by HOPE and presented in Fig. 5 are for the ionization state Al^{3+} .

The INFERNO code also uses average configuration occupations, and thereby computes the K -edge energy for an average ionization state. The single-particle energy levels and wave functions are also solved in a fully self-consistent manner using a Kohn-Sham local-density potential. The code uses an atomic model which assumes the atom embedded in an electron gas and requires the wave functions of the atom to decay exponentially (bound state) or to behave like normalized scattering state (free state) at the boundary at infinity. Bound states have discrete energies. When pressure-ionized the bound states turn into resonances in the continuum which broaden with further compression. This broadening of the excited levels into bands certainly occurs in a plasma at high density and low temperature.

However, it is not clear that this difference in the treatment of the boundary condition in HOPE and INFERNO will explain why they give different results for the K -edge energy shown in Fig. 5. Further work is certainly needed to clarify these results.

The augmented-plane-wave (APW) method widely used in band-structure calculations employs a muffin-tin approximation for the potential. In this case, the electron charge density in each unit cell is replaced by its spherical average within the inscribed sphere and by a constant in the interstitial region between the inscribed sphere and the unit cell boundary. The wave functions are expanded in linear combinations of "augmented" plane waves with expansion coefficients. In the interstitial region the form of the wave function is plane wave-like, while in the muffin-tin sphere region it consists of radial part and spherical harmonics consistent with the spherically symmetric potential. As only the APW wave functions (for two regions) and not their slopes are matched at the muffin-tin boundary, the expansion coefficients are determined variationally. This gives rise to a determinantal equation, the zeros of which are the energy eigenvalues. The APW calculations, being a self-consistent solid-state model, is considered to give the

most exact treatment of the dense-plasma effects. We can only conjecture that the apparent discrepancy with experimental observations may be due to the finite-temperature effect on the band structure calculation.

As noted above, the K -shell ionization energy of an isolated ion E_{IK} is strongly dependent on the ionic charge. The theoretical results described in Fig. 5 all correspond to an average ionization state of 3. If an ionization state of 4 were used, a blue shift in the K -edge energy would have been predicted by all models. Therefore, the experimental data has corroborated that the dominant ionization state in shock compressed aluminum remains at 3 up to twofold solid density. It should also be pointed out that in the ionization of a K -shell electron in an aluminum ion with a charge state of 3, both the initial and final states have single configurations. For ions with higher charge states, multiconfiguration calculations are required. For example, the possible states for Al^{4+} are $1s^2 2s^2 2p_{1/2}^2 2p_{3/2}^3 [j = \frac{3}{2}]$, $1s^2 2s^2 2p_{1/2} 2p_{3/2}^4 [j = \frac{1}{2}]$, and $1s^2 2s 2p_{1/2}^2 2p_{3/2}^4 [j = \frac{1}{2}]$. After the $1s$ electron is removed, the possible final states for the ion are $1s 2s 2p_{1/2}^2 2p_{3/2}^4 [j = 0]$, $1s 2s^2 2p_{1/2} 2p_{3/2}^4 [j = 0]$, $1s 2s 2p_{1/2}^2 2p_{3/2}^4 [j = 1]$, $1s 2s^2 2p_{1/2} 2p_{3/2}^4 [j = 1]$, and $1s 2s^2 2p_{1/2}^2 2p_{3/2}^4 [j = 2]$. The reason why there are more states after the removal of the $1s$ electron is due to the coupling between the $1s$ and $2s$ or $2p$ electrons. The multiconfiguration term-splitting treatment of the K edge is outside the scope of the present work.

Another important point to note is that in our model the K -edge energy is written as the K -shell ionization energy plus the electron degeneracy and continuum-lowering corrections. The ionization energies for the different aluminum ions presented in Table I are calculated using Hartree-Slater potentials for the ground-state configurations. The relaxation of the orbital energies and wave functions resulting from a photoionization transition is neglected in the calculation. To investigate such an effect on the ionization energy, we have calculated it as the difference of the total energies of the initial and final states of a photoionization transition. The total energy of a state is evaluated using the multiconfiguration Dirac-Fock code¹⁸ which treats explicitly the nonlocal exchange interaction between electrons. For Al^{3+} , we find that the K -shell ionization energy calculated as the difference of the total energies of the initial and final states is 1607.90 eV compared with 1584.0 eV given in Table I. Using the new value, we find that our model predicts the K -edge energy at normal condition to be 1584.68 eV rather than 1560.8 eV as is given in Fig. 4. However, the model would predict the same volume dependence of the K -edge energy as in Fig. 4. Therefore, the model still predicts the same amount of the shift in the K -edge energy under compression, although the absolute values will be different. When the K -shell ionization energies for the other aluminum ions are calculated as the difference of the total energies of the initial and final states of a photoionization transition, the new results will be different from these presented in Table I. Details of these calculations and the K -edge energy in a plasma predicted by the model using these new results are beyond

the scope of this paper and will be published elsewhere.

In conclusion, a phenomenological model has been constructed to assess dense-plasma effects on the K -shell photoabsorption-edge energy in aluminum. This model appears to overestimate the shift in the K -edge energy at high densities, while self-consistent calculations based on HOPE, INFERNO, or APW models describe apparently a lower bound of the dense-plasma effects. Further understanding of dependence of K -edge energy on density

would require more sophisticated models as well as more definitive measurement of the K -edge profile.

ACKNOWLEDGMENTS

We wish to thank A. K. McMahan for providing the APW calculations as well as enlightening discussions. This work is supported by the Natural Science and Engineering Research Council of Canada.

*Permanent address: Neutron Physics Division, Bhabha Atomic Research Centre, Bombay, India.

¹M. Ross, Rep. Prog. Phys. **68**, 1 (1985) and references therein.

²S. I. Anisimov, A. M. Prokhorov, and V. E. Fortov, Usp. Fiz. Nauk **142**, 395 (1984) [Sov. Phys.—Usp. **27**, 181 (1984)] and references therein.

³D. K. Bradley, J. Kilkeny, S. J. Rose, and J. D. Hares, Phys. Rev. Lett. **59**, 2995 (1987).

⁴T. A. Hall, A. Djaoui, R. W. Eason, C. L. Jackson, B. Shiwar, S. J. Rose, A. Cole, and P. Apte, Phys. Rev. Lett. **60**, 2034 (1988).

⁵L. Da Silva, A. Ng, B. K. Godwal, G. Chiu, F. Cottet, M. C. Richardson, P. A. Jaanimagi, and Y. T. Lee, Phys. Rev. Lett. **62**, 1623 (1989).

⁶B. F. Rozsnyai, Phys. Rev. A **5**, 1137 (1972).

⁷D. A. Liberman, Phys. Rev. B **20**, 4981 (1979).

⁸D. A. Liberman, J. Quant. Spectrosc. Radiat. Transfer **27**, 335 (1982).

⁹A. K. McMahan and M. Ross, *High Pressure Physics in Science and Technology* (Gordon and Breach, New York, 1968), Vol. 1.

¹⁰See, for example, D. D. Clayton, *Principles of Stellar Evolution and Nucleosynthesis* (McGraw-Hill, New York, 1968), p. 145.

¹¹V. Heine and D. Weaire, in *Solid State Physics*, edited by H. Ehrenrich, F. Seitz, and D. Turnbull (Academic, New York,

1970), Vol. 24.

¹²H. L. Skriver, *LMTO* (Springer-Verlag, Berlin, 1984).

¹³D. K. Bradley, J. Hares, A. Rankin, and S. J. Rose, Rutherford, Appleton Laboratory Report No. RAL-85-020, 1985 (unpublished).

¹⁴N. N. Kalitkin, Zh. Eksp. Teor. Fiz. **38**, 1534 (1960) [Sov. Phys.—JETP **11**, 1106 (1960)].

¹⁵C. A. Rouse, *Progress in High Temperature Physics and Chemistry* (Pergamon, New York, 1971), Vol. 4.

¹⁶B. K. Godwal, Phys. Rev. A **28**, 1103 (1983).

¹⁷F. Hermann and S. Skillman, *Atomic Structure Calculations* (Prentice-Hall, Englewood Cliffs, 1963), p. 10.

¹⁸I. P. Grant, B. J. McKenzie, P. H. Norrington, D. F. Mayere, and N. C. Pyper, Comput. Phys. Commun. **21**, 207 (1980).

¹⁹N. W. Ashcroft, Phys. Lett. **23**, 48 (1966).

²⁰W. Kohn and L. J. Sham, Phys. Rev. **140**, A1133 (1965).

²¹U. Von Barth and L. Hedin, J. Phys. C **5**, 1629 (1972).

²²B. L. Henke, P. Lee, T. J. Tanaka, R. L. Shimabukuro, and B. K. Fujikawa, At. Data Nucl. Data Tables **27**, 1 (1982).

²³J. C. Slater, *Self-consistent Field Calculation for Metals and Solids* (McGraw-Hill, New York, 1974), Vol. 4.

²⁴P. Celliers, Ph.D. thesis, University of British Columbia, 1988 (unpublished).

²⁵D. Duston, R. W. Clark, J. Davis, and J. P. Apruzese, Phys. Rev. A **27**, 1441 (1983).